Advances in Reliability, Safety and Security, Part 7 – Kołowrocki, Magryta-Mut (eds.)
 ISBN 978-83-68136-19-7 (printed), ISBN 978-83-68136-06-7 (electronic)

Advances in Reliability, Safety and Security

ESREL 2024
Monograph Book Series

Spatial Variability of Terrorist Vehicle Bomb Safety Risks

Mark G. Stewart

School of Civil and Environmental Engineering, University of Technology Sydney, Australia

Abstract

This paper describes results from an explosive field trial of the detonation of Vehicle Borne Improvised Explosive Devices (VBIEDs). The purpose of the trial is to replicate tests with identical car type and explosive mass to help probabilistically characterise the uncertainty and variability of blast pressures and fragment safety hazards. The paper describes the spatial variability (directionality) of incident pressure and impulse, and compares these to results from design and assessment software used for predicting blast loads from IEDs, such as ConWep. This also allows directional airblast factors to be quantified, and assess how this affects airblast fatality risks. Ultimately, probabilistic approaches will provide decision support for the determination of safety distance and risk reduction measures to prevent fatality and injury from blast pressure and fragmentation hazards.

Keywords: terrorism, VBIED, security, explosive blast, risk assessment, probability

1. Introduction

Improvised Explosive Devices (IEDs) have been a weapon of choice for terrorist attacks in Europe, North America and other western countries. Most IED attacks have involved (i) a Person-Borne Improvised Explosive Device (PBIED) or (ii) a Vehicle Borne IED (VBIED). Recent IED attacks include the attack on nightclubs in Bali (2002), Australian embassy in Jakarta (2004), Oslo government buildings (2011), Brussels airport and train station (2016), and Manchester Arena (2017). Added to this is the failed VBIED (car bomb) attack on Times Square and countless VBIED attacks on civilians and military personnel in Iraq, Afghanistan, Pakistan and elsewhere. People are highly vulnerable to VBIED attacks. VBIEDs comprise a large quantity of explosives, and produce primary fragments such as wheels, engine block, parts of door panels and other shrapnel that pose a serious safety hazard to people exposed in a street or other place of public assembly. Depending on the size and composition of a VBIED, fatalities can arise from blast overpressure within about 5-20 m of the VBIED, whereas primary fragments (car body and engine parts some weighing 10 kg or more) can cause fatalities hundreds of metres away. The most dangerous place to be is in the open – not in a building. Essential to this is an understanding of airblast and fragmentation variability (e.g., Qin and Stewart 2021).

The bulk explosives typically used for VBIEDs have to date been based mainly on a mixture of ammonium nitrate and fuel oil (so-called ANFO). The amount of explosives used in car bombs typically vary in size from 50 kg to 350 kg (FEMA 2011). However, according to Williams (2015) "***a review of open source media reports on bombing incidents around the world suggests that ... most vehicle-borne IEDs have a NEQ (net equivalent quantity) of less than 20 kg, a few in the hundreds of kg and very few in the tonnes.***" It is important to note that design threats specified by government and security organisations are often based on what is possible. Hence, according to Don Williams, "***Defining realistic NEQ is fundamental to appropriate protective structure advice. Consideration should be given to what is 'probable' rather than 'possible'***" (Williams 2015). This entails not using "***worse-case scenarios***." This is the approach taken herein. With this in mind, the United States Department of Defense recommends a VBIED threat of 100 kg for their buildings (UFC 4-010-02 2002).

The starting point for modelling blast and fragmentation casualty risks from VBIEDs is an explosive field trial. It should be noted that the Australian Government's Defence Science and Technology Group (DSTG) conducted three VBIED blast tests in 2011 comprising three different ANFO charges within three different vehicles

(Yokohama et al. 2015). Seven VBIED blast tests were also conducted in Europe (2006 – 2007) with charge masses up to 400 kg of PETN (Forsén et al. 2007, van der Voort and Rhijnsburger 2009). Similar trials have taken place in Poland (e.g., Sielicki et al. 2023). While these tests collected comprehensive data, the published tests (e.g., Yokohama et al. 2015) assumed symmetry about the main vehicle axis as they recorded blast pressures and fragmentation on only one side of the vehicle. The trials were not repeated, hence it is unknown how representative are the data obtained from only a single test for each charge mass/vehicle. In contrast, the field trial described herein will repeat each test three times to better capture airblast and fragment variability from VBIEDs.

The VBIED explosive field trial was conducted for three identical medium-sized cars. Explosive charge shape and location were identical for each vehicle, minimising test set-up variability. To record the directionality of blast pressures, eight incident pressure gauges will be set-up to record pressure-time histories for 45° azimuth intervals. Witness panels will record fragment velocity and density which can be used to help validate future stochastic models. This paper describes the spatial variability (directionality) of incident pressure and impulse, and compares these to results from the hemispherical surface burst Kingery and Bulmash (1984) polynomials often used for predicting blast loads from IEDs. Knowledge of the spatial distribution of blast loads is important for protective design, particularly for barriers and structures in the near-field and close to the source of the explosion, and also for casualty prediction. The paper also estimates the safety hazard risks from fragmentation. Finally, a primary motivation for the field trial is that the data and results presented herein can be used to help validate blast pressure models, fragment trajectory models, and other numerical or empirical predictive models.

2. Experimental Set-Up

A unique aspect of the field trial was the repeatability of tests. Considerable care was taken to ensure that vehicle location, explosive mass, detonator location, and the distance between the explosive and gauges were near identical for each test. Nonetheless, there will be some slight variability of these parameters.

A commercial range was used for the VBIED trial. The range is operated by RUREX Pty Ltd, and is licenced to acquire, handle, detonate and dispose of explosives. The location of the range is near Byrock in outback New South Wales in Australia, approximately 750 km from Sydney. The trial was conducted from 3-13 March 2023.

The range comprised a cleared flat area of approximately 250 m × 300 m – highly suitable when fragments are expected to travel several hundred metres from Ground Zero (GZ). Figure 1 shows an aerial image of the test range, where it is noted that several large trees may impede the trajectory of some fragments.

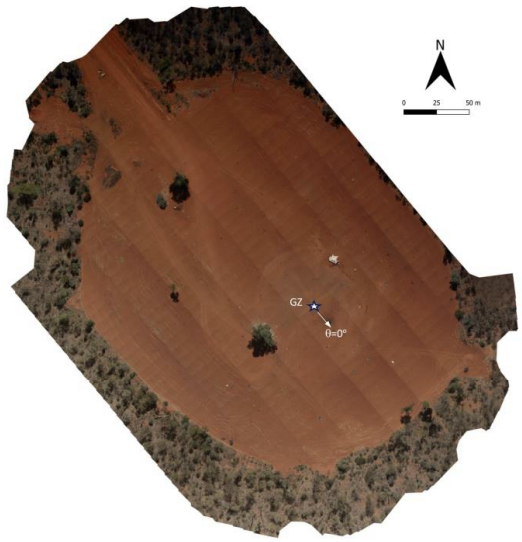

Fig. 1. Aerial image of the test range.

Three identical 2002 Toyota Camry vehicles were purchased and transported to the range. All hazardous materials from the engines and air-conditioning were then safely removed and disposed. However, 5L of petrol (fuel) was retained in each vehicle. To aid in identifying fragments from each vehicle, each vehicle was painted either red, white or blue including exteriors, interiors, engine compartment, boot, wheels, and undersides. The

vehicles were detonated in the same order – i.e., Shot 1 (Red), Shot 2 (White) and Shot 3 (Blue). Figure 2 shows the detonation of a VBIED. Each vehicle was orientated so the front faced θ=0°.

Fig. 2. Detonation of a VBIED (image courtesy of RUREX Pty. Ltd.).

To record the directionality of blast pressures, eight incident ground mounted pressure gauges were set-up to record pressure-time histories at 45° azimuth intervals around an 8 m radius from GZ (see Figures 3 and 4).

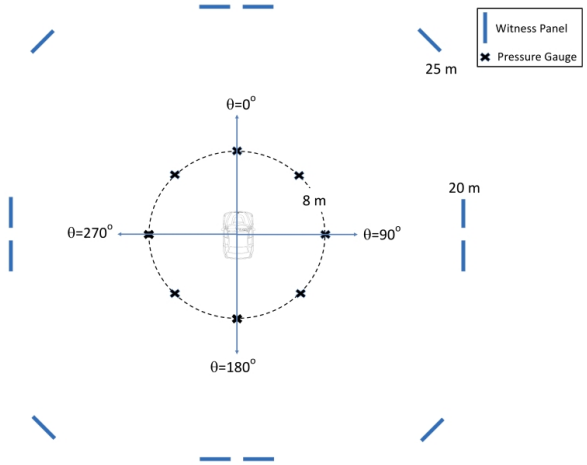

Fig. 3. Plan layout of blast gauges and witness panels at test arena where azimuth angle of 0° is directly in front of the vehicle.

Fig. 4. Ground mounted blast gauge located at 90°.

3. Results

During IED detonation the remaining body of each vehicle moved between 10-12 m from GZ in a 0° azimuth direction. In all cases the pressure gauge in that direction (8 m range) was untouched. Fragments after each shot were not collected, and so remained on the ground. Hence, the debris field was left undisturbed after each shot (see Figure 5), except for the car body that was removed after each shot. However, the debris field within the 8 m ranges consisted of relatively small fragments unlikely to affect the pressure wave as it reached the gauges, see for example, Figure 5 shows the debris field in front of the 0° pressure gauge.

Fig. 5. Photo of body of red vehicle and its location with respect to the blast gauge (3 m to the left of the car body).

3.1. Incident Pressure and Impulse

The detonation of high explosives releases a significant amount of energy, which heats up the immediate environment as well as producing gas. The violent expansion of these hot gases creates blast waves in any air surrounding the explosive. Figure 6 shows the pressure-time curve for the detonation of high explosives.

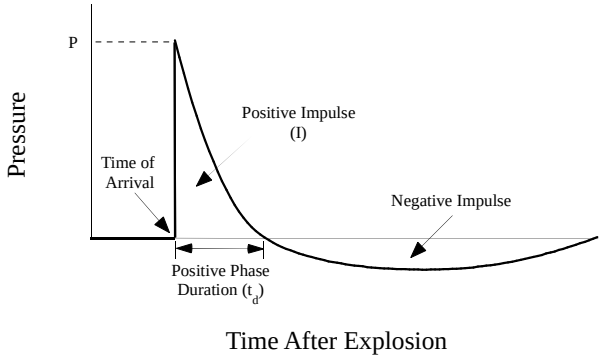

Fig. 6. Idealised Pressure-Time History Curve Showing Peak Incident Pressure (P) and Impulse (I).

3.2. Spatial Variability of Airblast

The observed spatial variability is probabilistically characterised by a directional airblast factor:

$$\text{Directional airblast factor} = \frac{\text{Observed (test) value for a specific direction and range}}{\text{Model prediction}} \quad (1)$$

Most, if not all, IED blast vulnerability studies assume that an explosive that detonates at, or very near to, the ground's surface will produce a hemispherical emanation of a blast wave away from the source that is unimpeded by the placement of the charge within the device. This provides the basis for the widely used ConWep (1991)

model. The ConWep model is based on the Kingery and Bulmash (1984) polynomials also widely used for casualty prediction, structural design and damage assessment (e.g., UFC 3-340-02 2014).

The peak incident pressure directional airblast factor for each gauge location and each shot is given in Figure 7 where ConWep predictions are corrected for temperature and atmospheric pressure at the time of testing. As expected, the peak incident pressure is lower than that predicted by the ConWep model (i.e., directional airblast factor is less than unity) due to the energy absorbing nature of a vehicle (e.g., Sunde et al. 2012). For instance, the pressures (or directional airblast factor) experienced in front of the vehicle tend to be lower than from the side or rear of the car as the engine block is more likely to impede and absorb energy than the energy required to rupture thin-walled door panels.

The incident pressures opposite the doors of the vehicle (90°, 270°) results in mean directional airblast factor of 0.81 – i.e., a 19% reduction. This was also observed from a series of three VBIED tests of differing charges masses conducted by the DSTG (Sunde et al. 2012) found that airblast incident pressures were 12-25% lower when measured at one side of vehicle.

As shown in Figure 7 and Table 1 the mean and COV are dependent on vehicle orientation. This spatial variable will be more noticeable nearer GZ, and is expected to be less noticeable as the blast wave emanates and coalesces further from the source of detonation (e.g., Sunde et al. 2012).

Table 1. Directional airblast factors for ConWep (1991).

	Peak Incident Pressure		Incident Impulse	
Direction	Mean	COV	Mean	COV
0°	0.76	0.05	0.90	0.02
45°	0.78	0.03	0.82	0.02
90°	0.77	0.06	0.81	0.02
135°	0.90	0.06	0.75	0.05
180°	0.78	0.08	0.61	0.03
225°	0.83	0.12	0.76	0.04
270°	0.85	0.13	0.81	0.03
315°	0.71	0.03	0.82	0.03

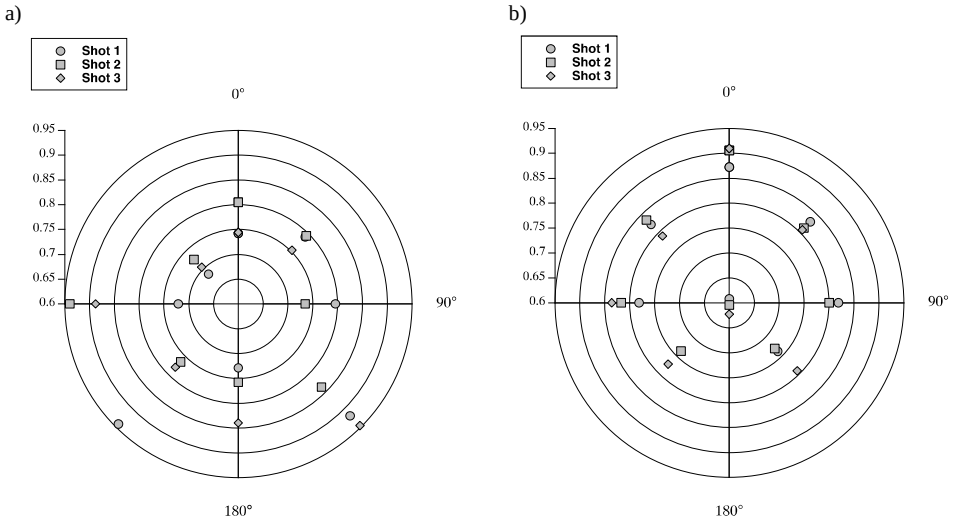

Fig. 7. Directional airblast factors for (a) peak incident pressure and (b) incident impulse.

The spatial distribution of directional airblast factor for incident impulse is also shown in Figure 7. In this case, the impulse is higher directly in front of the vehicle as while the engine block will interrupt the peak incident pressure, it will impede the arrival of the blast wave leading to a longer time of positive arrival hence leading to a higher impulse. This observation also applies to some other directions, namely a higher impulse is associated with a higher time of positive arrival, due most likely to higher impedance of the blast wave.

The COVs of test measurements compare favourably against previous repetitive field tests under controlled conditions. For example, Stewart et al. (2020) found that the COV for measured incident pressure, impulse and time of positive phase duration using an above ground baffle plate the varied from 0.03 to 0.12 for each shot. This provides some confidence that the ground mounted gauges performed satisfactorily.

Some of the measurements and their variability may be due to non-ideal conditions such as the ground surface not being perfectly level, blast wave may be impeded by small fragments on the ground, etc. However, the overall trends seem reasonable.

If the test or measurement uncertainty (variation in the measured values due to the accuracy of instrumentation, measured range, mass, etc.) is taken as ±5-10% (i.e., COV is 0.025 to 0.05), then the inherent (or aleatory) variability (natural, intrinsic, irreducible random uncertainty of a situation) will produce a COV 0.01 to 0.05 lower than those shown in Table 1. In other words, the inherent variability of blast loading will be relatively low for most directions.

The source of the spatial variability is due to: (i) vehicle parts and components not being symmetrical within the vehicle (e.g., driver console is on one side of the vehicle), (ii) variability of component strengths, (iii) inherent spatial variability of shock wave emanating from an explosion(e.g., Stewart 2023), etc.

3.3. Human Vulnerability to Airblast

An IED may cause direct damage to the human body primarily to the ears and lungs and the body (i.e. impacting hard surfaces), due to the impacts of the pressure front of the blast wave itself. The probability of fatality ($P_{f\text{-airblast}}$) from airblast is estimated as a function of peak pressure (P), total impulse (I), and mass of the human body taken as 70 kg (DDESB 2009, TNO 1992, Mannan 2012, Giannopoulos et al. 2010). The three fatality risk elements are:

(i) lung rupture ($P_{f(lr)}$),
(ii) whole body displacement ($P_{f(bd)}$), and
(iii) skull fracture ($P_{f(sf)}$).

The probability of airblast fatality ($P_{f\text{-airblast}}$) is:

$$P_{f-airblast} = 1 - \left(1 - P_{f(lr)}\right)\left(1 - P_{f(bd)}\right)\left(1 - P_{f(sf)}\right) \quad (2)$$

If the threat scenario is a terrorist VBIED comprised of 500 kg of ANFO, then Figure 8 shows the airblast fatality risks for a person located 12 m from the vehicle. A conventional risk assessment would predict a near 100% fatality risk in every direction around the VBIED. However, this is conservative. If the airblast directional factors given in Table 1 are used to better characterise P and I, then Figure 8 shows that fatality risks reduce significantly by at least 61%, and by as much as 99.9% for the rear of the vehicle (180°).

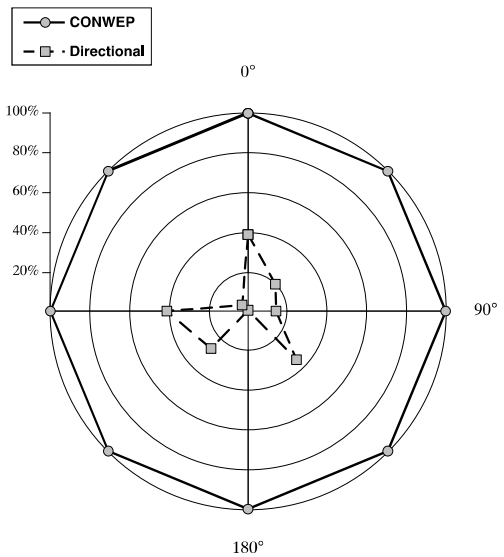

Fig. 8. Airblast fatality risks for 500 kg VBIED at 12 m.

4. Spatial Variability of Fragmentation Hazards

Figure 9 shows several fragments impacting the witness screens (1.23 m high × 2.45 m long) with velocities of up to 800 m/s.

Fig. 9. Fragments impacting a witness panel.

Aerial drone footage was used to recorded fragment counts. In this case 20,393, 6,283 and 156 fragments were recorded for those with dimensions less than 1 cm to 10 cm, 10 cm to 1 m, and over 1 m, respectively – a total of 26,832 fragments. In other words, each VBIED test generated approximately 8,950 fragments that were visible (>1 cm) in the test arena.

Figure 10 shows the fragment densities per m^2 for dimensions less than 1 cm to 10 cm. It is observed that there is considerable spatial variability in the fragment distribution, and fragment density close to GZ can exceed 10 fragments per m^2. Table 2 shows the total fragment count (> 1 cm) in a 5 m wide strip in eight directions for fragments located 25 m away from GZ. While symmetry of fragments counts might be expected, for example, at 45° and 315°, the total number of <1 cm fragments in these directions are 123 and 391, respectively, a difference of 69%. Similar differences are observed for other directions where symmetry of results might be expected. It might have been expected that after three shots some "averaging" of fragment distribution shown in Table 2 would be observed. However, this is not observed further emphasising the highly spatial nature of fragment throw for each shot.

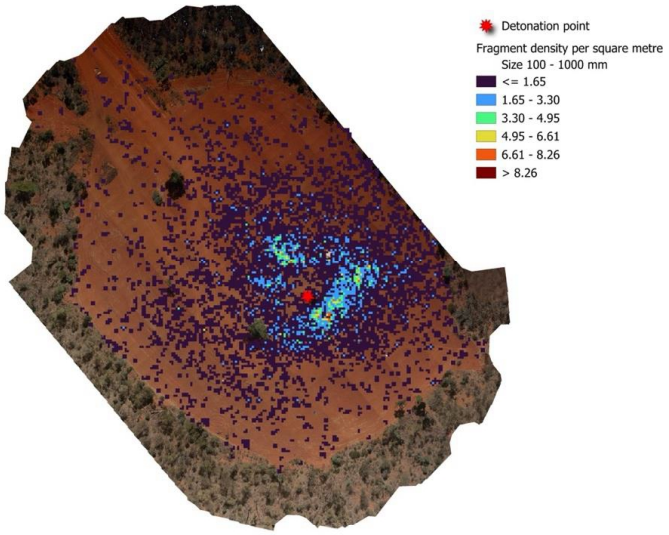

Fig. 10. Fragment densities for fragments 1 cm to 10 cm in length.

Fragment trajectory angle, density and velocity are still being estimated from the VBIED trial data. Hence, the following is a procedure to estimate fatality risks, where most of the probabilistic information is assumed for based on overall test observations.

Trajectory angle and fragment density may be treated as a bivariate distribution for vertical (θ_x) and horizontal (azimuth) (θ_y) trajectory angles (e.g., Sielicki et al. 2021). As the data for the VBIED trial is still being analysed, for convenience assume that the trajectory angle θ_x is uniformly distributed between 0^o and 45^o. Moreover, the number of fragments in each direction at a distance exceeds 25 m (see Table 2) is assumed uniformly distributed over the 5 m width. For an average standing person (i.e., 1.75m tall) the exposed critical body area A_P is 0.50 m^2 facing the detonation point (Qin and Stewart 2021, DDESB 2009). At a short distance of 25 m it is appropriate to use a line-of-sight approach because, at high speeds, the fragments will travel in approximately a straight line over short distances. It follows that the average number of fragments (N_R) impacting a standing person 25 m from the VBIED can be calculated, as is shown in Table 2. As expected, the higher the number of fragments generated for each direction the higher is N_R. The probability of being hit (P_{hit}) by at least one fragment is deduced from the Poisson distribution:

$$P_{hit} = 1 - \exp[-N_R] \tag{3}$$

Table 2 shows that P_{hit} is 43% higher for a person standing behind the VBIED than it is for someone standing directly in front.

Table 2. Fragment count in a 5 m strip and probability of a person being hit at 25 m from VBIED.

	0°	45°	90°	135°	180°	225°	270°	315°
Fragments	195	123	153	189	454	291	548	391
N_R	0.99	0.63	0.78	0.96	2.31	1.48	2.79	1.99
P_{hit}	63.0%	46.6%	54.1%	61.8%	90.1%	77.3%	93.9%	86.3%

The probability of fatality is a function of the kinetic energy (KE) of a fragment hitting an average standing person is modelled by a lognormal function:

$$\Pr(\text{fatality}|H) = \Phi\left[\frac{ln(KE)-\mu_{ln}}{\sigma_{ln}}\right] \tag{4}$$

where H is the hazard (fragments), Φ is cumulative distribution function of a standard normal distribution, and μ_{ln}=4.662 and σ_{ln}=0.5536 are parameters that are estimated based on the weighted average of head, thorax, abdomen and limb fatality vulnerabilities for an average standing person facing the detonation point (Qin and Stewart 2021, DDESB 2009). Figure 11 shows the vulnerability curve for fatalities and injuries. For example, if the fragments with the highest recorded velocity (800 m/s) are a mere 2 g in mass then KE is 640J. A larger fragment of 20 g but slower one at 200 m/s still retains a high KE of 400J and in both circumstances would be fatal if struck. When probabilistic knowledge on fragment mass and velocity are inferred, then fatality risks can be estimated (e.g., Qin and Stewart 2021). This information will be inferred from the VBIED trial and estimation of casualty risks and safe evacuation distances is the subject of future research.

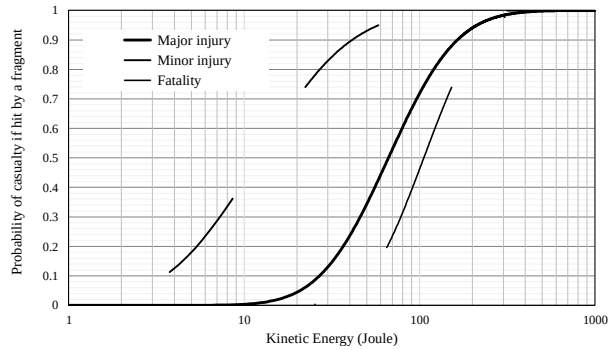

Fig. 11. Vulnerability curves for an average standing person if hit by a fragment (Qin and Stewart 2021).

Summary

An explosive field trial was conducted where repetitive testing comprising three identical VBIEDs were detonated to help statistically characterise the uncertainty and variability of blast pressures and fragment hazards. Incident pressure and impulse were recorded, and mean and variability of directional airblast factors were estimated when compared to the ConWep model often used for protective design. As expected, the energy absorbing nature of the vehicle was highest directly in front of the vehicle. Witness screens enabled fragment densities and velocities to be recorded, with the highest fragment velocity being 800 m/s. Finally, the spatial distribution of over 26,000 fragments on the ground was also presented over the 250 m × 300 m test arena, and preliminary estimates of casualty risks presented. These data will help develop or validate airblast and fragmentation hazard models.

Acknowledgements

The assistance of Dr Michael Netherton from MAJAM Pty. Ltd., Ryan Esam and Peter Doyle from RUREX Pty Ltd; Dr Hao Qin and Mable Fong from the University of Technology Sydney; Michael Goodwin, Ross Gibson, Kevin Khuu, Andy Sullivan, Dr Michele Spadari, Associate Professor Klaus Thoeni, and Dr Lloyd Pilgrim from The University of Newcastle; Professor Alex Remennikov from The University of Wollongong; and the folks from the Mulga Creek Hotel in Byrock are all greatly appreciated. The support from the Australian Research Council Discovery Project DP210101487 is also gratefully acknowledged.

References

ConWep 1991. *Conventional Weapons Effects Program*, Prepared by D.W. Hyde, US Waterways Experimental Station, Vicksburg.

DDESB 2009. *Approved Methods and Algorithms for DoD Risk-Based Explosives Siting*, Department of Defense Explosives Safety Board, , Alexandria, VA, USA.

FEMA 2011. *Reference Manual to Mitigate Potential Terrorist Attacks Against Buildings*, FEMA 426, Washington, DC, October 2011.

Forsén, R., Magnusson, J., van der Voort, M. and Rhijnsburger, M. 2007. Physical protection against VBIED threats, *12th International Symposium on the Interaction of the Effects of Munitions with Structures*, Orlando, U.S.

Giannopoulos, G., Larcher, M., Casadei, F. and Solomos, G. 2010. Risk Assessment of the Fatality Due to Explosion in Land Mass Transport Infrastructure by Fast Transient Dynamic Analysis, *Journal of Hazardous Materials*, 173(1-3): 401-408.

Kingery, C. N., and Bulmash, G. 1984. *Airblast parameters from TNT spherical air burst and hemispherical surface burst*. U.S. Army Armament Research and Development Center, Aberdeen Proving Ground, MD.

Mannan, S. 2012). *Lees' Loss Prevention in the Process Industries*, Butterworth-Heinemann, Amsterdam.

Qin, H. and Stewart, M. G. 2021. Casualty risks induced by primary fragmentation hazards from high-explosive munitions. *Reliability Engineering & System Safety*, 215, 107874.

Sielicki, P.W., Stewart, M.G., Gajewski, T., Malendowski, M., Peksa, P., Al-Rifaie, H., Studziński, R. and Wojciech, S. 2021. Field Test and Probabilistic Analysis of Irregular Steel Debris Casualty Risks from a Person-Borne Improvised Explosive Device, *Defence Technology*, 17(6): 1862-1863.

Sielicki, P.W., Gajewski, G., et al. 2023. Prediction of the Flying Fragments Trajectories After VBIED Detonation *26th International Symposium on Military Aspects of Blast and Shock (MABS26)*, Wollongong, Australia, Paper 104.

Stewart, M.G., Baldacchino, H. and Netherton, M.D. 2020. Observed Airblast Variability and Model Error from Repeatable Explosive Field Trials, *International Journal of Protective Structures*, 11(2): 235–257.

Stewart, M.G. 2023. Spatial Variability of Explosive Blast Loading and its Effect on Damage Risks to Reinforced Concrete Buildings, *Engineering Structures*, 285: 115650.

Sunde, J., Burman, N. and Hart, R. 2012. VBIED Blast Pressures - Comparison of Predicted and Measured Results, *Australian Structural Engineering Conference ASEC2012*, The Past, Present and Future of Structural Engineering, Perth.

TNO 1992. *Methods for the Determination of Possible Damage to People and Objects Resulting from Releases of Hazardous Materials (TNO Green Book)*, CPR 16E, Directorate-General of Labour of the Ministry of Social Affairs and Employment, The Hague, The Netherlands.

UFC 4-010-02 2002. *Minimum Antiterrorism Standards For Buildings*, US Department of Defense, Washington, D.C., 29 May 2002.

UFC 3-340-02 2014. *Structures to Resist the Effects of Accidental Explosions*, Unified Facilities Criteria, UFC 3-340-02, Department of Defense, Washington D.C.

UN 2015. I*nternational IATG Ammunition Technical 02.20 Guideline: Quantity and separation distances*, United Nations, New York.

van der Voort, M. and Rhijnsburger, M. 2009. IED effects research at TNO Defence Security and Safety, *13th International Symposium on the Interaction of the Effects of Munitions with Structures*, Bruhl, Germany.

Williams, D. 2015. Enhancing the Applicability of Blast Modelling and Advice, *International Journal of Protective Structures*, 6(4): 701-709.

Yokohama, H., Sunde, J., Ellis-Steinborne and Ayubi, Z. 2015. Vehicle Borne Improvised Explosive Device (VBIED) Characterisation and Estimation of its Effects in Terms of Human Injury, *International Journal of Protective Structures*, 6(4): 607-627.